

Letter Report

Yucca Mountain Environmental Monitoring Systems Initiative
Air Quality Scoping Study for Beatty, Nevada



prepared by

Johann Engelbrecht, Ilias Kavouras, Dave Campbell,
Scott Campbell, Steven Kohl and David Shafer
Desert Research Institute
Nevada System of Higher Education

submitted to

Nevada Site Office
National Nuclear Security Administration
U.S. Department of Energy
Las Vegas, Nevada

April 2007

The work upon which this report is based was supported by the U.S. Department of Energy under Contract #DE-AC52-06NA26383.

CONTENTS

LIST OF FIGURES	iii
LIST OF TABLES	iv
INTRODUCTION	1
SITE LOCATION AND CHARACTERISTICS	1
AEROSOL SAMPLING AND MONITORING	2
Filter Sampling	2
Sampler Description and Procedures	2
Gravimetry	4
Chemical Analysis	6
Aerosol Monitoring	10
Monitor Description and Procedures	10
Continuous Measurements of PM ₁₀ and PM _{2.5}	12
Comparison of Filter to Continuous Results	16
METEOROLOGY	18
Associations of Meteorology with Aerosol Measurements	22
CONCLUSIONS	24
ACKNOWLEDGEMENTS	25
REFERENCES	25

LIST OF FIGURES

1. Southern Nevada map showing the location of Site #2 (at Beatty), Nevada Test Site, and Yucca Mountain	1
2. Location of the mobile trailer in Beatty, NV. Image obtained from Google Earth	2
3. Photographs of PQ100 (green/gray box in left photo), PQ200 (white box in left photo) and their sampling inlet (right photo)	3
4. A diagrammatic representation of the BGI PM _{2.5} sampler showing the PM ₁₀ size selective impactor head as the first stage followed by a PM _{2.5} VSCC.	3
5. Time series of PM ₁₀ and PM _{2.5} mass concentrations (mean ± uncertainty) at Site #2 (Beatty)	5
6. Relationship between mean (± uncertainty) daily PM _{2.5} and PM ₁₀ at Beatty	6
7. Reconstructed mass for PM ₁₀ and PM _{2.5} based on chemical composition.	10
8. Left photograph: The front panels of PM ₁₀ (right on the left photograph) and PM _{2.5} (left on the left photograph) of TEOM. Right photograph: The measurement units of TEOM and DUSTTRAK on top of them.	11
9. Sampling inlet for DUSTTRAK	12
10. Mean 24-h PM ₁₀ and PM _{2.5} mass concentrations measured by TEOM at Site #2 (Beatty) ...	13
11. PM _{2.5} /PM ₁₀ mass ratios at Site #2 (Beatty)	13
12. Variation of mean (± st.error) PM ₁₀ and PM _{2.5} (µg/m ³) in weekdays and weekends at Site #2 (Beatty) (Monday=1, Tuesday=2, Wednesday=3, Thursday=4, Friday=5, Saturday=6, Sunday=7)	14

13. PM ₁₀ mass (µg/m ³) measured with DUSTTRAK and TEOM at Site #2 (Beatty).....	15
14. PM _{2.5} mass (µg/m ³) measured with DUSTTRAK and TEOM at Site #2 (Beatty).....	15
15. Comparison of 24-h PM ₁₀ and PM _{2.5} mass concentrations measured by TEOM and DUSTTRAK. Error bars represent the standard error of the mean.	16
16. Relationships between PM ₁₀ concentrations (µg/m ³) measured by TEOM, DUSTTRAK, and filter-based methods.	17
17. Relationships between PM _{2.5} concentrations (µg/m ³) measured by TEOM, DUSTTRAK, and filter-based methods.	17
18. Solar radiation (in watts/m ²) at Site #2 (Beatty).....	18
19. Temperature (in °F) and relative humidity at Site #2 (Beatty).	19
20. Total precipitation (in mm) at Site #2 (Beatty).....	19
21. Wind speed (in miles/hr) at Site #2 (Beatty).	20
22. Wind direction at Site #2 (Beatty).	20
23. Wind direction and speed at Beatty.	21
24. Average wind speed for each wind direction sector.	22
25. Hourly variation of PM ₁₀ and PM _{2.5} mass concentrations (µg/m ³) as well as wind speed (miles/hour) at Site #2 (Beatty).....	23
26. Mean (± st.error) of PM ₁₀ mass concentrations (µg/m ³) for different wind direction sectors at Site #2 (Beatty).	23
27. Mean (± st.error) of PM _{2.5} mass concentrations (µg/m ³) for different wind direction sectors at Site #2 (Beatty).	24

LIST OF TABLES

1. Longitude, latitude, and elevation of the mobile trailer location at Site #2 Beatty.	2
2. Collection day, filter number, mass, and uncertainty determined by gravimetric analysis and associated flags of samples at Site #2 (Beatty).	5
3. Results of the chemical analysis for selected filters from Beatty.	6
4. Statistics for 24-h PM ₁₀ and PM _{2.5} TEOM mass concentrations.	12
5. Descriptive statistics of 1-hour meteorological data.	18
6. Wind condition classifications.	21

INTRODUCTION

The Desert Research Institute (DRI) is performing a scoping study as part of the U.S. Department of Energy's Yucca Mountain Environmental Monitoring Systems Initiative (EMSI). The main objective is to obtain baseline air quality information for Yucca Mountain and an area surrounding the Nevada Test Site (NTS).

Air quality and meteorological monitoring and sampling equipment housed in a mobile trailer (shelter) is collecting data at seven sites outside the NTS, including Ash Meadows National Wildlife Refuge, Sarcobatus Flat, Beatty, Rachel, Caliente, Pahrnagat National Wildlife Refuge, and Crater Flat, and at four sites on the NTS. The trailer is stationed at any one site for approximately eight weeks at a time.

Letter reports provide summaries of air quality and meteorological data, on completion of each site's sampling program.

SITE LOCATION AND CHARACTERISTICS

The town of Beatty is located in the Amargosa River Valley in Nye County, Nevada ($36^{\circ}51'34''\text{N}$, $116^{\circ}45'16''\text{W}$ at 3,320 feet in elevation). It has a population of 1,154 inhabitants. Beatty is the nearest town to the Yucca Mountain Repository facility, 18 miles to the east (Figure 1), and to Death Valley National Park. The climate is characterized by hot summers, cool winters, and less than 5 inches of rain annually.

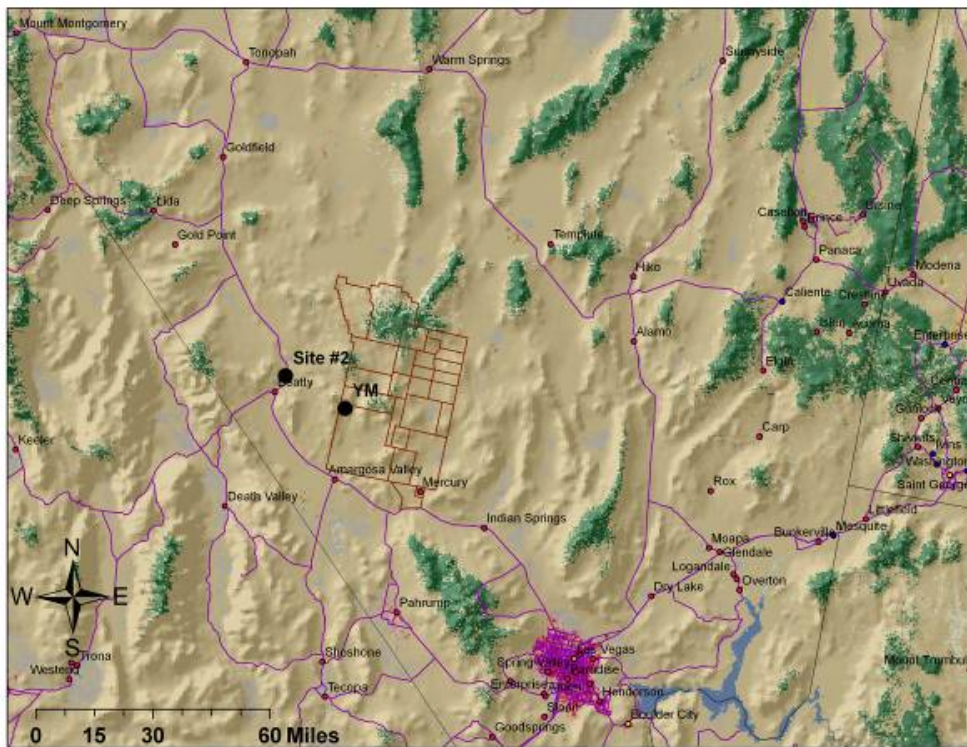


Figure 1. Southern Nevada map showing the location of Site #2 (at Beatty), Nevada Test Site, and Yucca Mountain. The map background is land use and land cover obtained from the 2001 National Land Cover Database.

The mobile trailer was located on private property 5 miles north of Beatty along U.S. Highway 95 (Figure 2). Monitoring of PM₁₀, PM_{2.5}, and meteorological conditions was carried out from May 19, 2006, to July 05, 2006.

Table 1. Longitude, latitude, and elevation of the mobile trailer location at Site #2 (Beatty).

Site	Beatty
Latitude	36° 58' 19"
Longitude	116° 43' 33"



Figure 2. Location of the mobile trailer in Beatty, NV. Image obtained from Google Earth.

AEROSOL SAMPLING AND MONITORING

Filter Sampling

Sampler Description and Procedures

BGI, Inc., PQ100 and PQ200 Ambient PM_{2.5} Federal Reference Method (FRM) samplers were used to collect 24-h integrated PM₁₀ and PM_{2.5} samples. Figure 3 shows the PQ100 and PQ200 in the mobile trailer (left) and the PM₁₀ sampling inlets on the top of the trailer (right). Both PQ100 (Designation No. RFPS-1298-124) and PQ200 (Designation No. RFPS-0498-116) are designed to meet the criteria for collecting 24-h samples of ambient aerosol according to the U.S. National Ambient Air Quality Standards (NAAQS).

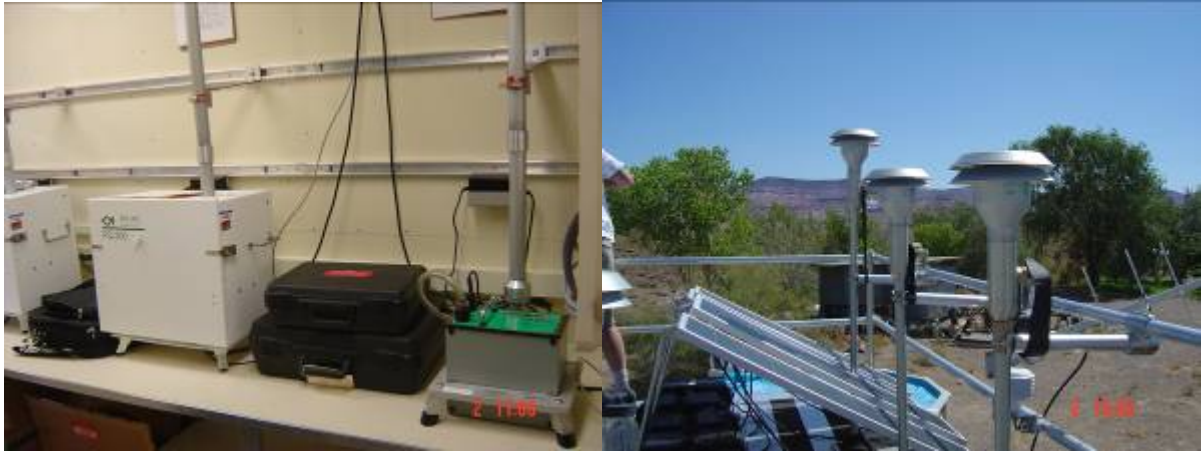


Figure 3. Photographs of PQ100 (green/gray box in left photo), PQ200 (white box in left photo) and their sampling inlet (right photo).

Figure 4 shows a schematic drawing of the samplers. Briefly, particles with aerodynamic diameter larger than $10\ \mu\text{m}$ were removed by impaction at the size selective inlet, while the remaining particles remained airborne. For the PM_{10} fraction, particles were then collected by a filter located downstream of the size selective inlet. For the collection of $\text{PM}_{2.5}$, particles in the range between 2.5 and $10\ \mu\text{m}$ were removed by the Very Sharp Cut Cyclone (VSCC) (U.S. Environmental Protection Agency [EPA] Equivalent Designation No. EQPM-0202-142), then collected by a filter.

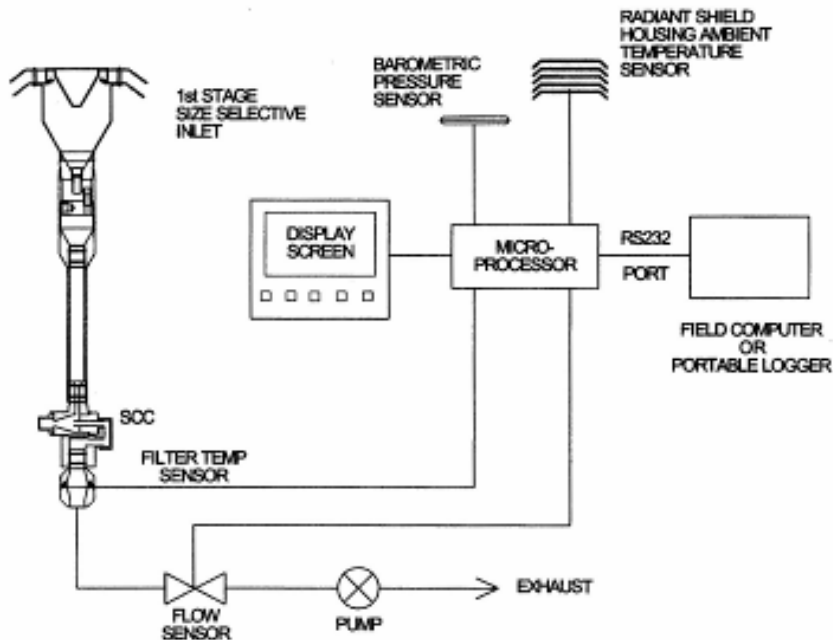


Figure 4. A diagrammatic representation of the BGI $\text{PM}_{2.5}$ sampler showing the PM_{10} size selective impactor head as the first stage followed by a $\text{PM}_{2.5}$ VSCC. This configuration can be readily modified to a PM_{10} sampler by removal of the VSCC.

For both the PQ100 and PQ200, samples were collected at a volumetric flow rate of 16.67 liters/min. The flow rate is controlled to ± 2 percent precision with a mass flow meter. The actual ambient temperature and barometric pressure, filter temperature and pressure, and anomalies (if any) were recorded (and controlled) by a microprocessor. The sampler was equipped to operate from an internal 12-volt DC battery. The battery was recharged by a battery charger from 120-volt AC. Alternatively, a 32-watt solar panel with an additional external ballast battery was installed to provide power for days without electricity. Two sets of PQ100 and PQ200 samplers were installed in the mobile trailer. PM_{10} and $PM_{2.5}$ samples were collected on filters in numbered cassettes, labeled TT (for PM_{10} Teflon), FT (for $PM_{2.5}$ Teflon), TQ (for PM_{10} Quartz), and FQ (for $PM_{2.5}$ Quartz). Each filter cassette was loaded with a pre-weighed 46.2-mm-diameter PTFE (Teflon) membrane filter (Whatman # 7592-004) or 47-mm quartz fiber (Pallflex #2500QAT-UP) filter. The Teflon membrane collected particles for measurement of mass by gravimetric analysis, light absorption by densitometry, and elements by x-ray fluorescence spectrometry. Quartz fiber filters were used for measurement of water-soluble ions by atomic absorption spectrometry, ion chromatography, and automated colorimetry, and also for measurement of carbon species by thermal optical reflectance.

Operation, calibration, and maintenance of PQ100 and PQ200 are described in standard operation procedure (SOP) "BGI PQ100 PM_{10} and PQ200 $PM_{2.5}$ REFERENCE SAMPLERS FOR THE YUCCA MOUNTAIN AIR QUALITY PROGRAM." Flow calibration and leak tests were performed on the day of installation (May 18, 2006). The leak check was performed according to the manufacturer's operational instruction manual only for PQ200; no procedure exists for the PQ100. The flow rate was calibrated using a BGI Tri-Cal flow meter. The sampler was then placed in calibration or "run" mode and a one-point calibration verification or one-point flow-rate verification was performed. Aerosol samples were collected on a 1-in-6-day schedule. Audits of the flow and leak tests were done onsite at the beginning and end of the monitoring campaign. Teflon and quartz filters were prepared and assembled in their filter holders in the Desert Research Institute's (DRI) Environmental Analysis Facility (EAF) in Reno and shipped to DRI's facilities in Las Vegas. The filters were kept at $-4^{\circ}C$ and transported to the field in a cryo-cooler. Exposed filters were also stored at $-4^{\circ}C$ in Las Vegas. Upon completion of the monitoring period at the site, all filters were shipped to the EAF in Reno.

Gravimetry

Table 2 shows mass concentrations (and uncertainty) for filters collected at Beatty. PM_{10} mass concentrations varied from $8.94 \mu g/m^3$ to $23.00 \mu g/m^3$, while $PM_{2.5}$ mass concentrations ranged from $2.25 \mu g/m^3$ to $9.07 \mu g/m^3$. Similar temporal trends were observed for both PM_{10} and $PM_{2.5}$. In all cases, 24-h PM_{10} and $PM_{2.5}$ levels were substantially lower than the daily and annual NAAQS as recently revised by EPA (24-h PM_{10} : $150 \mu g/m^3$, 24-h $PM_{2.5}$: $35 \mu g/m^3$; Annual $PM_{2.5}$: $15 \mu g/m^3$) (Figure 5). Fine particles ($PM_{2.5}$) accounted for approximately one-third of PM_{10} ($PM_{2.5}/PM_{10}$ ratio of 0.35) (Figure 6). This value was indicative of the predominant contribution of coarse particles sources (e.g., dust), with some impact of anthropogenic sources (e.g., combustion, vehicle emissions) from traffic on U.S. Highway 95 and the town of Beatty, which is located about 5 miles south of the site.

Table 2. Collection day, filter number, mass, and uncertainty determined by gravimetric analysis and associated flags of samples at Site #2 (Beatty).

Date	No	Type	Mass ($\mu\text{g}/\text{m}^3$)	Uncertainty ($\mu\text{g}/\text{m}^3$)	Flags
5/23/2006	16	PM ₁₀	9.9084	0.5252	f: Teflon membrane separated from support ring q: sampling time > 25 hours
		PM _{2.5}	2.4979	0.4889	
5/29/2006	17	PM ₁₀	9.6922	0.5232	
		PM _{2.5}	2.2472	0.4882	
6/4/2006	19	PM ₁₀	15.3494	0.5748	
		PM _{2.5}	3.5387	0.4915	
6/10/2006	20	PM ₁₀	20.3997	0.6348	
		PM _{2.5}	6.9052	0.5052	
6/16/2006	21	PM ₁₀	8.9434	0.5178	
		PM _{2.5}	2.7466	0.4892	
6/20/2006	22	PM ₁₀	9.1930	0.5196	
6/28/2006	23	PM _{2.5}	5.6659	0.1583	
		PM ₁₀	17.8453	0.6029	
7/4/2006	25	PM _{2.5}	9.0720	0.5189	
		PM ₁₀	23.0033	0.6692	
		PM _{2.5}	7.0329	0.5061	

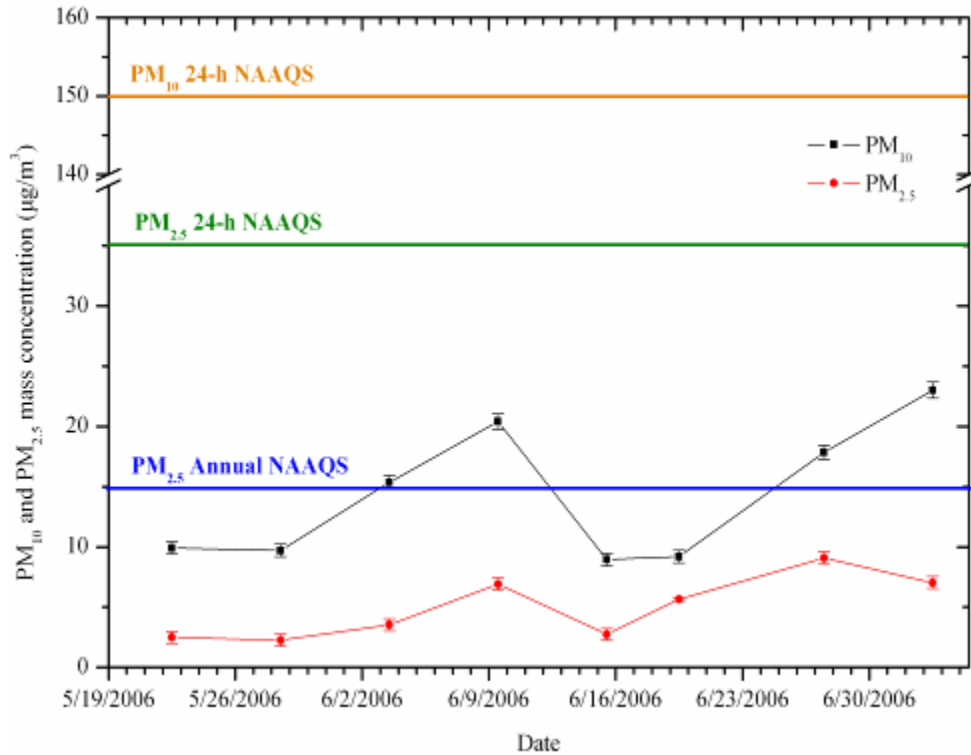


Figure 5. Time series of PM₁₀ and PM_{2.5} mass concentrations (mean \pm uncertainty) at Site #2 (Beatty).

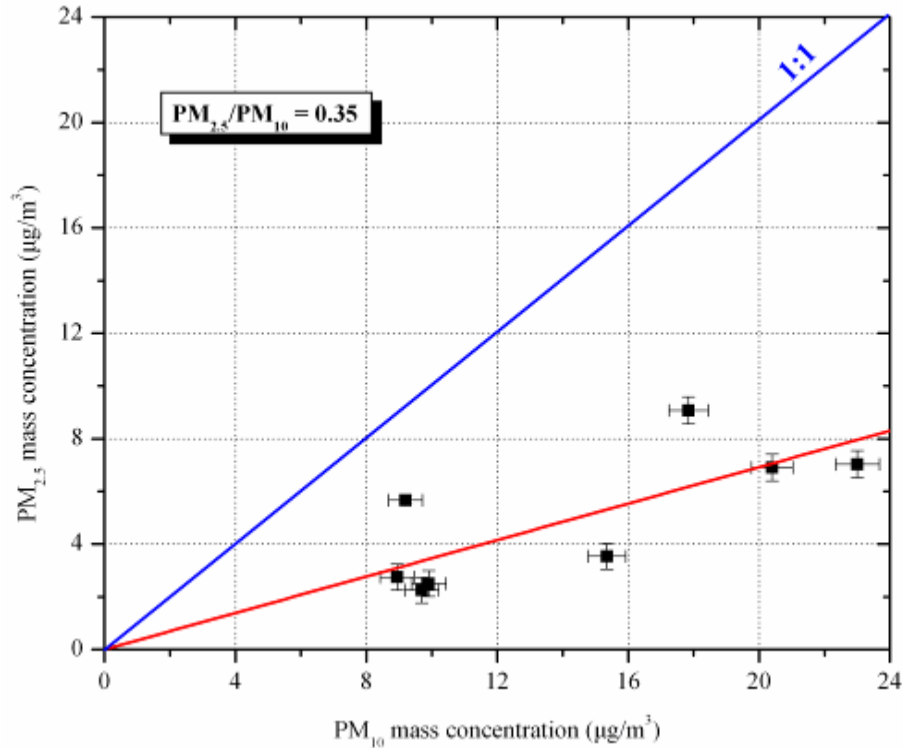


Figure 6. Relationship between mean (\pm uncertainty) daily $PM_{2.5}$ and PM_{10} at Beatty.

Chemical Analysis

Table 3 shows the chemical content of PM_{10} and $PM_{2.5}$ samples collected on 6/04/2006 and 6/28/2006. Chemical analysis included elements (from sodium to uranium) with x-ray fluorescence spectrometry, major anions (sulfate, nitrate, and chloride) by ion chromatography, major cations (sodium, potassium) by atomic absorption, particulate ammonium by colorimetry, and elemental and organic carbon by thermal optical reflectance (TOR).

Table 3. Results of the chemical analysis for selected filters from Beatty. Chemical components with concentration higher than two times the uncertainty are in bold, while those with concentrations lower than two times the uncertainty are in italics. Concentrations are in $\mu\text{g}/\text{m}^3$.

DATE SIZE	6/04/2006				6/28/2006			
	PM_{10}		$PM_{2.5}$		PM_{10}		$PM_{2.5}$	
	Conc.	Uncer.	Conc.	Uncer.	Conc.	Uncer.	Conc.	Uncer.
Chloride, Cl^-	<i>0.0513</i>	<i>0.0298</i>	<i>0.0075</i>	<i>0.0294</i>	<i>0.0216</i>	<i>0.0295</i>	<i>0.0086</i>	<i>0.0294</i>
Nitrate, NO_3^-	0.1937	0.0297	0.0664	0.0295	0.3307	0.0302	0.1684	0.0296
Sulfate, SO_4^{2-}	1.0662	0.0367	0.7305	0.0331	1.2866	0.0396	1.3958	0.0411
Ammonium, NH_4^+	0.2371	0.0309	0.2397	0.0309	0.4631	0.0343	0.5151	0.0354
Sodium, Na^+	0.2078	0.0047	0.0245	0.0018	0.0897	0.0026	0.0861	0.0025
Potassium, K^+	0.1158	0.0061	0.0196	0.0031	0.1149	0.0061	0.0985	0.0055

Table 3. Results of the chemical analysis for selected filters from Beatty. Chemical components with concentration higher than two times the uncertainty are in bold, while those with concentrations lower than two times the uncertainty are in italics. Concentrations are in $\mu\text{g}/\text{m}^3$ (continued).

DATE SIZE	6/04/2006				6/28/2006			
	PM ₁₀		PM _{2.5}		PM ₁₀		PM _{2.5}	
	Conc.	Uncer.	Conc.	Uncer.	Conc.	Uncer.	Conc.	Uncer.
OC1	1.8108	0.2797	1.9449	0.3002	1.5386	0.2379	1.9755	0.305
OC2	2.1487	0.4055	1.7073	0.3247	1.4655	0.2805	1.4196	0.2721
OC3	1.3156	0.2289	0.9253	0.1982	1.4966	0.2447	1.237	0.2224
OC4	0.6395	0.1727	0.3514	0.1041	0.7919	0.2107	0.6069	0.1647
Pyrolyzed OC-TT	0.7873	0.1626	0.3567	0.0807	1.0169	0.2078	1.1221	0.2287
Pyrolyzed OC-Op	0.6941	0.1345	0.24	0.058	0.9032	0.1722	1.0166	0.1929
Total OC	6.6064	0.7538	5.1666	0.6059	6.1936	0.7111	6.2533	0.7173
EC1	0.6703	0.1389	0.24	0.0561	1.1766	0.2404	1.1458	0.2342
EC2	0.1801	0.0472	0.1391	0.0426	0.2103	0.0509	0.2502	0.0563
EC3	0	0.0116	0	0.0116	0	0.0116	0	0.0116
Total EC	0.1562	0.067	0.1391	0.0629	0.4837	0.1626	0.3794	0.1304
Total Carbon	6.7626	0.4944	5.3057	0.4125	6.6772	0.4895	6.6326	0.4869
Sodium, Na	0.1916	0.1521	<i>0</i>	<i>0.1487</i>	<i>0.1</i>	<i>0.1507</i>	<i>0.0544</i>	<i>0.1501</i>
Magnesium, Mg	0.1983	0.0457	0.067	0.0449	0.2218	0.0458	0.0675	0.0449
Aluminum, Al	0.6163	0.0236	0.1381	0.0184	0.6148	0.0236	0.1974	0.0188
Silicon, Si	1.7414	0.0413	0.326	0.0166	1.512	0.0368	0.4597	0.0183
Phosphorous, P	0.0256	0.0046	0.0159	0.0046	0.0291	0.0046	0.0222	0.0046
Sulfur, S	0.4144	0.0221	0.3323	0.0214	0.5359	0.0232	0.5504	0.0234
Chlorine, Cl	0.0399	0.0038	0	0.0037	0.0134	0.0037	<i>0.0021</i>	<i>0.0037</i>
Potassium, K	0.3411	0.0072	0.0574	0.0023	0.3249	0.0069	0.1338	0.0034
Calcium, Ca	0.591	0.0123	0.126	0.0038	0.6988	0.0145	0.152	0.0042
Scandium, Sc	<i>0</i>	<i>0.0074</i>	<i>0</i>	<i>0.0074</i>	<i>0.0003</i>	<i>0.0074</i>	<i>0</i>	<i>0.0074</i>
Titanium, Ti	0.0405	0.0016	0.0062	0.0013	0.0415	0.0016	0.0092	0.0013
Vanadium, V	<i>0</i>	<i>0.0003</i>	<i>0.0002</i>	<i>0.0003</i>	<i>0</i>	<i>0.0003</i>	<i>0.0007</i>	<i>0.0003</i>
Chromium, Cr	<i>0.0002</i>	<i>0.0015</i>	<i>0.0007</i>	<i>0.0015</i>	<i>0.0007</i>	<i>0.0015</i>	<i>0.0002</i>	<i>0.0015</i>
Manganese, Mn	<i>0.0126</i>	<i>0.0032</i>	<i>0.0057</i>	<i>0.0032</i>	<i>0.0082</i>	<i>0.0032</i>	<i>0.0057</i>	<i>0.0032</i>
Iron, Fe	0.3985	0.0088	0.087	0.0037	0.4108	0.009	0.1163	0.0041
Cobalt, Co	<i>0</i>	<i>0.0003</i>	<i>0</i>	<i>0.0003</i>	<i>0</i>	<i>0.0003</i>	<i>0</i>	<i>0.0003</i>
Nickel, Ni	<i>0</i>	<i>0.0008</i>	<i>0.001</i>	<i>0.0008</i>	<i>0.0005</i>	<i>0.0008</i>	<i>0.0015</i>	<i>0.0008</i>
Copper, Cu	<i>0</i>	<i>0.0017</i>	<i>0.0003</i>	<i>0.0017</i>	<i>0</i>	<i>0.0017</i>	<i>0.0003</i>	<i>0.0017</i>
Zinc, Zn	<i>0.0029</i>	<i>0.0015</i>	<i>0.0005</i>	<i>0.0015</i>	0.0039	0.0015	<i>0.0015</i>	<i>0.0015</i>
Gallium, Ga	<i>0.0015</i>	<i>0.0049</i>	<i>0.0034</i>	<i>0.0049</i>	<i>0.0034</i>	<i>0.0049</i>	<i>0</i>	<i>0.0049</i>
Arsenic, As	<i>0</i>	<i>0.0006</i>	<i>0</i>	<i>0.0006</i>	<i>0</i>	<i>0.0006</i>	<i>0.0005</i>	<i>0.0006</i>
Selenium, Se	<i>0</i>	<i>0.0011</i>	<i>0</i>	<i>0.0011</i>	<i>0</i>	<i>0.0011</i>	<i>0</i>	<i>0.0011</i>
Bromine, Br	<i>0.0003</i>	<i>0.0021</i>	<i>0.0018</i>	<i>0.0021</i>	<i>0.0047</i>	<i>0.0021</i>	<i>0.0043</i>	<i>0.0021</i>
Rubidium, Rb	0.0026	0.0011	<i>0</i>	<i>0.001</i>	<i>0.0007</i>	<i>0.0011</i>	<i>0.0002</i>	<i>0.0011</i>
Strontium, Sr	0.0059	0.0025	<i>0.0025</i>	<i>0.0025</i>	0.0064	0.0025	<i>0.0005</i>	<i>0.0025</i>
Yttrium, Y	<i>0</i>	<i>0.0015</i>	<i>0.0007</i>	<i>0.0015</i>	<i>0.0007</i>	<i>0.0015</i>	<i>0.0002</i>	<i>0.0015</i>
Zirconium, Zr	<i>0.0008</i>	<i>0.0039</i>	<i>0.0018</i>	<i>0.0039</i>	<i>0</i>	<i>0.0039</i>	<i>0.0018</i>	<i>0.0039</i>
Niobium, Nb	<i>0</i>	<i>0.0025</i>	<i>0</i>	<i>0.0025</i>	<i>0</i>	<i>0.0025</i>	<i>0</i>	<i>0.0025</i>
Molybdenum, Mo	<i>0</i>	<i>0.0025</i>	<i>0.0008</i>	<i>0.0025</i>	<i>0.0008</i>	<i>0.0025</i>	<i>0</i>	<i>0.0025</i>

Table 3. Results of the chemical analysis for selected filters from Beatty. Chemical components with concentration higher than two times the uncertainty are in bold, while those with concentrations lower than two times the uncertainty are in italics. Concentrations are in $\mu\text{g}/\text{m}^3$ (continued).

DATE SIZE	6/04/2006				6/28/2006			
	PM ₁₀		PM _{2.5}		PM ₁₀		PM _{2.5}	
	Conc.	Uncer.	Conc.	Uncer.	Conc.	Uncer.	Conc.	Uncer.
Palladium, Pd	<i>0.001</i>	<i>0.0059</i>	<i>0</i>	<i>0.0059</i>	<i>0.0064</i>	<i>0.0059</i>	<i>0</i>	<i>0.0059</i>
Silver, Ag	<i>0.006</i>	<i>0.0056</i>	<i>0.0016</i>	<i>0.0056</i>	<i>0.0036</i>	<i>0.0056</i>	<i>0</i>	<i>0.0056</i>
Cadmium, Cd	<i>0</i>	<i>0.0044</i>	<i>0</i>	<i>0.0044</i>	<i>0</i>	<i>0.0044</i>	<i>0.0008</i>	<i>0.0044</i>
Indium, In	<i>0</i>	<i>0.0048</i>	<i>0</i>	<i>0.0049</i>	<i>0</i>	<i>0.0049</i>	<i>0</i>	<i>0.0049</i>
Tin, Sn	<i>0</i>	<i>0.0053</i>	<i>0</i>	<i>0.0053</i>	<i>0.0028</i>	<i>0.0053</i>	<i>0.0003</i>	<i>0.0053</i>
Antimony, Sb	<i>0.0051</i>	<i>0.008</i>	<i>0</i>	<i>0.008</i>	<i>0.0041</i>	<i>0.008</i>	<i>0</i>	<i>0.008</i>
Cesium, Cs	<i>0</i>	<i>0.0023</i>	<i>0</i>	<i>0.0023</i>	<i>0</i>	<i>0.0023</i>	<i>0</i>	<i>0.0023</i>
Barium, Ba	<i>0</i>	<i>0.0025</i>	<i>0.0026</i>	<i>0.0025</i>	<i>0.0031</i>	<i>0.0025</i>	<i>0</i>	<i>0.0025</i>
Lanthanum, La	<i>0</i>	<i>0.0017</i>	<i>0</i>	<i>0.0017</i>	<i>0.0003</i>	<i>0.0017</i>	<i>0</i>	<i>0.0017</i>
Cerium, Ce	<i>0.0003</i>	<i>0.0016</i>	<i>0</i>	<i>0.0016</i>	<i>0.0003</i>	<i>0.0016</i>	<i>0</i>	<i>0.0016</i>
Samarium, Sa	<i>0.002</i>	<i>0.0033</i>	<i>0</i>	<i>0.0033</i>	<i>0.002</i>	<i>0.0033</i>	<i>0.0015</i>	<i>0.0033</i>
Europium, Eu	<i>0</i>	<i>0.0051</i>	<i>0</i>	<i>0.0051</i>	<i>0</i>	<i>0.0051</i>	<i>0</i>	<i>0.0051</i>
Terbium, Tb	<i>0.0005</i>	<i>0.0037</i>	<i>0</i>	<i>0.0038</i>	<i>0</i>	<i>0.0038</i>	<i>0</i>	<i>0.0037</i>
Hafnium, Hf	<i>0</i>	<i>0.0152</i>	<i>0</i>	<i>0.0152</i>	<i>0.0047</i>	<i>0.0152</i>	<i>0.0008</i>	<i>0.0152</i>
Tantalum, Ta	<i>0</i>	<i>0.0099</i>	<i>0</i>	<i>0.0099</i>	<i>0</i>	<i>0.0099</i>	<i>0.002</i>	<i>0.01</i>
Tungsten, W	<i>0.0005</i>	<i>0.0164</i>	<i>0.0059</i>	<i>0.0164</i>	<i>0</i>	<i>0.0164</i>	<i>0</i>	<i>0.0164</i>
Iridium, Ir	<i>0.0005</i>	<i>0.0046</i>	<i>0</i>	<i>0.0046</i>	<i>0</i>	<i>0.0046</i>	<i>0</i>	<i>0.0046</i>
Gold, Au	<i>0</i>	<i>0.0075</i>	<i>0</i>	<i>0.0075</i>	<i>0</i>	<i>0.0075</i>	<i>0</i>	<i>0.0075</i>
Mercury, Hg	<i>0</i>	<i>0.0037</i>	<i>0</i>	<i>0.0037</i>	<i>0</i>	<i>0.0037</i>	<i>0</i>	<i>0.0037</i>
Thallium, Th	<i>0</i>	<i>0.0025</i>	<i>0</i>	<i>0.0025</i>	<i>0</i>	<i>0.0025</i>	<i>0</i>	<i>0.0025</i>
Lead, Pb	<i>0</i>	<i>0.0036</i>	<i>0.0008</i>	<i>0.0036</i>	<i>0.0023</i>	<i>0.0036</i>	<i>0.0033</i>	<i>0.0036</i>
Uranium, U	<i>0</i>	<i>0.0063</i>	<i>0.0031</i>	<i>0.0063</i>	<i>0</i>	<i>0.0063</i>	<i>0.0021</i>	<i>0.0063</i>

OC = organic carbon
 EC = elemental carbon
 OP = optical pyrolysis
 TT = transmittance

With respect to the chemical composition of PM₁₀ and PM_{2.5}, the following patterns are observed:

- Sulfur (S) was mostly in the form of sulfate (SO₄²⁻) with sulfate-to-sulfur ratio of 2.19 to 2.57. Sulfate and ammonium were almost entirely (70 to 100% for sulfate, 100% for ammonium) associated with fine particles, while less than 50 percent of nitrate (34 to 50%) was measured in PM_{2.5}. Ammonium-to-sulfate molar ratios varied from 1.18 to 1.96, suggesting that sulfate aerosol was mostly in the form of ammonium bisulfate, (NH₄)HSO₄ (Malm *et al.*, 2002). Nitrates appeared to be partially neutralized by ammonium in the fine-particle mode, while coarse-particle nitrates may be the product of the reactions of nitric acid with soil dust elements such as Ca (Lefer and Talbot, 2001).
- Carbonaceous aerosol was predominantly in fine particles. For PM_{2.5}, organic carbon (OC) concentrations accounted for more than 70 percent of particle mass. This may

be attributed to the positive bias of OC concentrations caused by the absorption of low vapor pressure organic compounds on the quartz filter. Overestimation also may explain the relatively low EC/OC ratio values (between 0.03 and 0.08), which were approximately 10 times lower than those determined for atmospheric aerosol.

- Soluble potassium (K^+) accounted for one-third of total potassium in PM_{10} and 30 to 70 percent of total potassium in $PM_{2.5}$. Soluble potassium is a tracer of biomass burning, which suggested the impact of emissions from local and/or regional fire (prescribed or wildfires) events. This was further supported by estimates of non-soil potassium $K_{\text{non-soil}} (K_{\text{total}} - (0.26 \times [Al]))$ that were comparable to measured water-soluble K^+ .
- Ratios of Al/Si (0.35 to 0.43) Ca/Al (0.77 to 1.13) were comparable to those determined for samples collected at the Interagency Monitoring of Protected Visibility Environments (IMPROVE) sites in the western United States (Al/Si: 0.31 to 0.43, Al/Ca: 1.4 to 1.7) when soil dust was the major component of particulate matter (Kavouras *et al.*, 2005)], while the relatively high K/Fe (0.65 to 1.15) indicated the contribution of biomass burning, in agreement with the concentration levels of soluble potassium.

The IMPROVE mass estimation scheme is adopted to reconstruct aerosol mass into five major types: sulfate, nitrate, organic, light-absorbing carbon, and soil. For this scheme, sulfate and nitrate are assumed to be in the forms of ammonium sulfate $[(NH_4)_2SO_4]$ and ammonium nitrate $[NH_4NO_3]$, respectively (Malm *et al.*, 2004). Organic mass concentration [OMC] was estimated as $[OMC] = 1.4 \times [OC]$, where [OC] is the organic carbon concentration. The 1.4 factor was used to correct for other elements (mainly hydrogen and oxygen) associated with the composition of organic compounds (White and Roberts, 1977). Soil mass concentration [SOIL] was estimated as the sum of the elements present in the soil as oxides (Al_2O_3 , SiO_2 , CaO , K_2O , FeO , Fe_2O_3 , and TiO_2) as follows:

$[SOIL] = 2.2 \times [Al] + 2.49 [Si] + 1.63 \times [Ca] + 2.42 \times [Fe] + 1.94 \times [Ti]$. Therefore, the reconstructed aerosol mass was estimated as follows:

$$[\text{Aerosol Mass}] = (128/96) \times [SO_4] + (80/62) \times [NO_3] + EC + [OMC] + [SOIL]$$

Figure 7 shows the concentrations of ammonium sulfate, ammonium nitrate, organic carbon mass, elemental carbon, and soil for PM_{10} and $PM_{2.5}$ collected on 6/04/2006 and 6/28/2006 in Beatty. Considering the positive bias for organic carbon measurements:

- Reconstructed particle mass accounted for 102 to 123 percent of measured PM_{10} mass and for 148 to 283 percent of $PM_{2.5}$ mass.
- Carbonaceous aerosol (OMC and EC) appeared to account for 50 percent of PM_{10} and 68 to 74 percent of $PM_{2.5}$.
- Soil represented 40 percent of PM_{10} and about 15 percent of $PM_{2.5}$ mass, while sulfate contributed about 9 percent for PM_{10} and 12 percent for $PM_{2.5}$ (Figure 7).
- Although, the differences of PM_{10} fractions for the two days were negligible, higher $PM_{2.5}$ mass concentrations for the second day (June 28, 2006) may be attributed to higher concentrations of organic carbon.

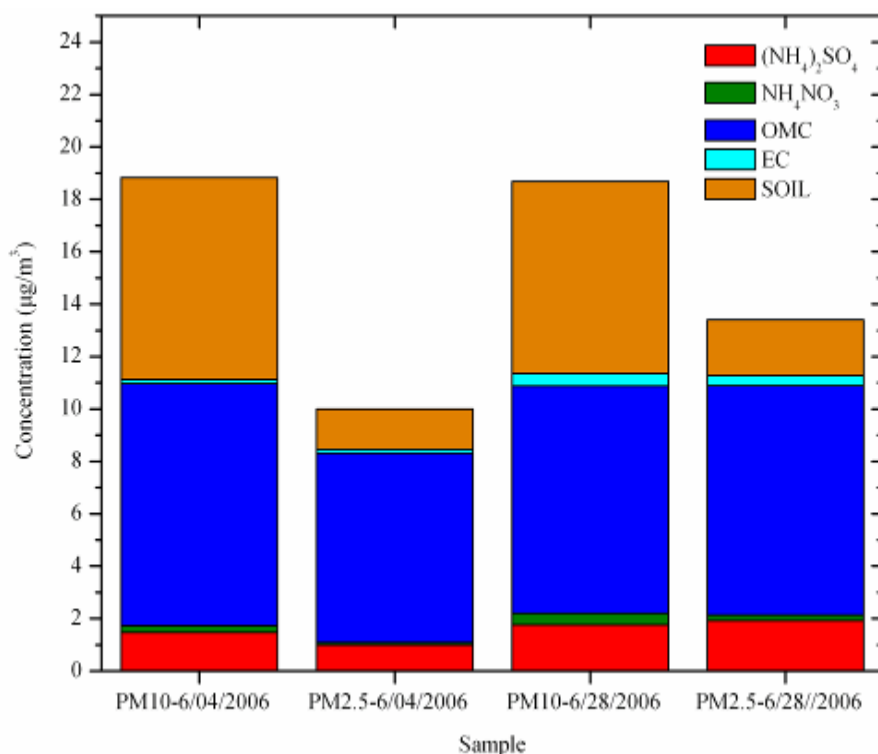


Figure 7. Reconstructed mass for PM₁₀ and PM_{2.5} based on chemical composition.

Aerosol Monitoring

Monitor Description and Procedures

The TEOM Series 1400 Ambient Particulate Monitor from Thermo Scientific and the DUSTTRAK™ Aerosol Monitor from TSI were used to continuously measure PM₁₀ and PM_{2.5} mass concentrations (Figure 8). The TEOM Series 1400 monitors the ambient particulate mass concentration of PM₁₀ (EPA certification EQPM-1090-079) (or PM_{2.5}) in real time by direct measurement of particulate mass collected on a filter attached to an oscillating inertial mass transducer. The mass transducer in the sensor unit has a tapered ceramic tube (element) that is fixed at the downstream end and a Teflon-coated glass fiber filter on the free end. The oscillating frequency of the tube changes proportionally as ambient air is drawn through the filter and the particulate loading thereon increases. The flow-rate through the filter sample is set at a nominal 3.0 l/min. A bypass (auxiliary) flow provides an additional 13.67 l/min for a total flow rate of 16.67 l/min. An internal datalogger stores mass values, time, and some meteorological data. To eliminate bias caused by humidity, the filter is heated to 50°C. Operation, calibration, and maintenance of the TEOM is described in SOP “RUPPRECHT & PATASHNICK (R&P), SERIES 1400A TAPERED ELEMENT OSCILLATING MICROBALANCE (TEOM).” Flow calibration and leak tests were performed on the day of installation (May 18, 2006). Data were downloaded during site visits. Regular checks of time, filter loading, by-pass filter, and flow rates were accomplished during site visits.



Figure 8. Left photograph: The front panels of PM₁₀ (right on the left photograph) and PM_{2.5} (left on the left photograph) of TEOM. Right photograph: The measurement units of TEOM and DUSTTRAK on top of them.

The DUSTTRAK™ Aerosol Monitor is a portable, battery operated laser photometer. The monitor provides measurements of particle mass based on 90° light scattering. Atmospheric aerosol passes through a size selective inlet (either PM₁₀ or PM_{2.5}) and is directed to an optics chamber at a flow rate of 1.7 l/min. The light source is a laser diode that emits light at a wavelength of 780 nm. The aerosol sample is drawn into the sensing chamber where it is illuminated with a narrow beam of laser light. Light scattered by aerosol particles is collected by a set of lenses and focused onto the photodetector. The detector signal is proportional to the amount of scattered light, which is proportional to the mass concentration of the aerosol. Voltage is read by the processor and multiplied by an internal calibration constant to yield mass concentration. The calibration constant is pre-set by the manufacturer for scattering characteristics of the respirable mass of ISO 12103-1, Al test dust. Local variations in aerosol particle size distribution and composition relative to this standard may result in differences in the actual response factor of the instrument. The operation, calibration, and maintenance of TSI is described in SOP “TSI INCORPORATED MODEL 8520 DUSTTRAK AEROSOL MONITOR FOR THE YUCCA MOUNTAIN AIR QUALITY PROGRAM.”

Both PM₁₀ and PM_{2.5} DUSTTRAK inlets were attached on a wide “Y” connector, which was connected to one end of a second “Y” (Figure 9). A funnel was connected to the other end of the second “Y” to achieve fast exchange of ambient air into the sampling line. Flow calibration and zero-tests were performed on the day of installation (March 24, 2007) and subsequent site visits. Deviations in flow were predominantly due to failure of the pump diaphragm. In those cases, the instrument was replaced. Deviations of the zero check were corrected by performing zero calibration according to the manufacturer’s operational instruction manual.

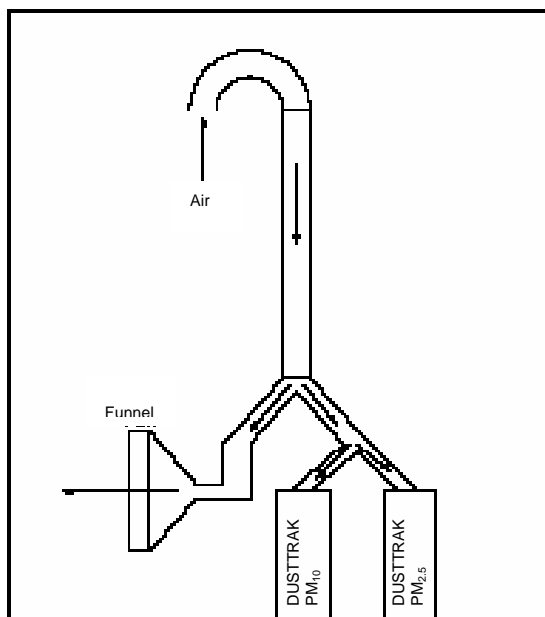


Figure 9. Sampling inlet for DUSTTRAK.

Continuous Measurements of PM₁₀ and PM_{2.5}

Trends and correlations of particle mass are examined using hourly TEOM data integrated for 24 hours (from 0:00. to 23:00). Statistics of 24-h particle mass are presented in Table 4. Twenty-four-h PM₁₀ levels ranged from 9.3 to 38.5 $\mu\text{g}/\text{m}^3$, with a mean of 19.7 ($\sigma = 5.9$) $\mu\text{g}/\text{m}^3$, while PM_{2.5} concentrations varied from 1.0 to 10.6 $\mu\text{g}/\text{m}^3$, with a mean of 4.6 ($\sigma = 2.1$) $\mu\text{g}/\text{m}^3$.

Table 4. Statistics for 24-h PM₁₀ and PM_{2.5} TEOM mass concentrations.

	Mean	Median	Minimum	Maximum	Std. Deviation
PM ₁₀	19.7	19.7	9.3	38.5	5.9
PM _{2.5}	4.6	4.8	1.0	10.6	2.1

A consistent relationship between PM fractions was observed during the monitoring period, with fine particles being accounted for about one-fourth of PM₁₀ (PM_{2.5}/PM₁₀ ratio of 0.24) (Figure 11). While differences in particle mass for weekdays/weekends were not statistically significant, somewhat lower PM₁₀ and PM_{2.5} levels were measured on Thursday (Day #4), and the highest on Saturday (Day #6) (Figure 12). The pattern was more pronounced for PM₁₀ as compared to PM_{2.5}. This may be due to the increased traffic on U.S. Highway 95 because of visitors to Death Valley National Park during the weekends.

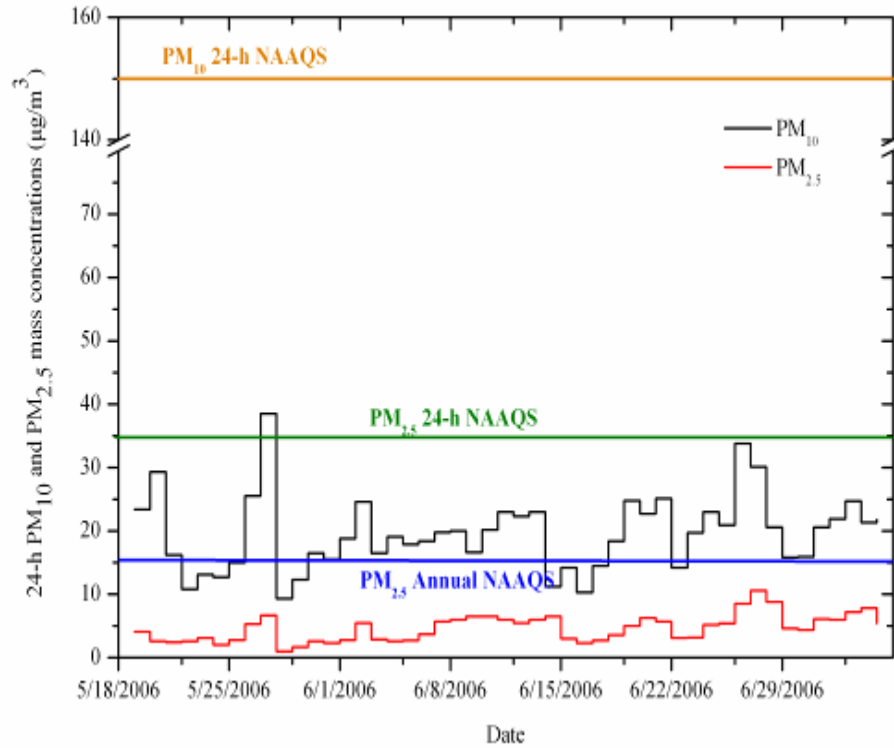


Figure 10. Mean 24-h PM_{10} and $PM_{2.5}$ mass concentrations measured by TEOM at Site #2 (Beatty).

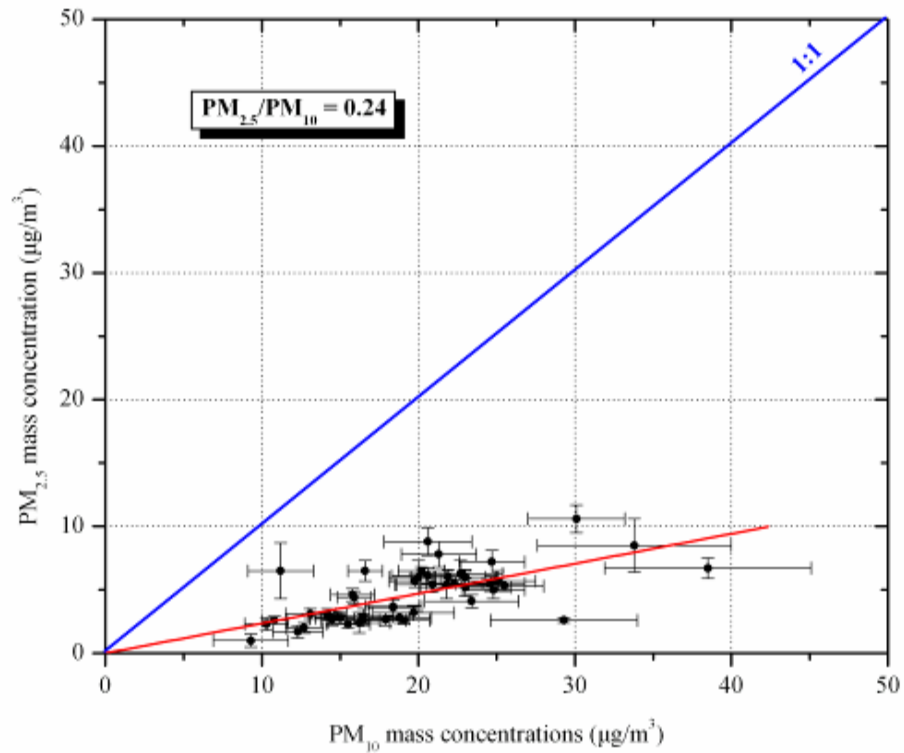


Figure 11. $PM_{2.5}/PM_{10}$ mass ratios at Site #2 (Beatty). Error bars represent the standard error of the mean.

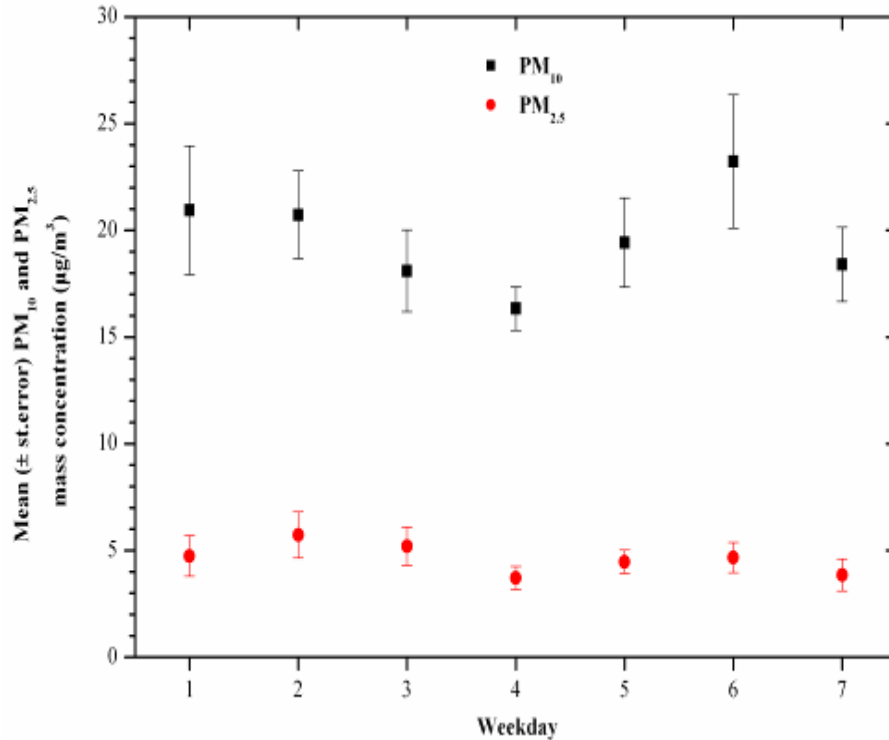


Figure 12. Variation of mean (\pm st.error) PM₁₀ and PM_{2.5} ($\mu\text{g}/\text{m}^3$) in weekdays and weekends at Site #2 (Beatty) (Monday=1, Tuesday=2, Wednesday=3, Thursday=4, Friday=5, Saturday=6, Sunday=7).

Variations of daily PM₁₀ and PM_{2.5} measured with the DUSTTRAK and TEOM are presented in Figure 13 and Figure 14. The time series plots for PM₁₀ particle mass concentrations measured by TEOM and DUSTTRAK are somewhat comparable in shape and almost identical for PM_{2.5}. A rather poor correlation of PM₁₀ concentrations measured by TEOM and DUSTTRAK was observed, with a slope of 0.25885 and an intercept of 2.54885 $\mu\text{g}/\text{m}^3$ (Figure 15). This was indicative of the weakness of the light scattering technique to monitor dust particles that represented more than 70 percent of PM₁₀ mass in Beatty. As for PM_{2.5}, both TEOM and DUSTTRAK were quite comparable, the slope between TEOM and DUSTTRAK PM_{2.5} was 0.95514, with a rather low intercept of 0.68414 $\mu\text{g}/\text{m}^3$. This good agreement was due to the fact that light scattering provides more reliable measurements of particle mass in the accumulation mode, while losses of volatile species such as nitric acid and low vapor organic compounds were negligible.

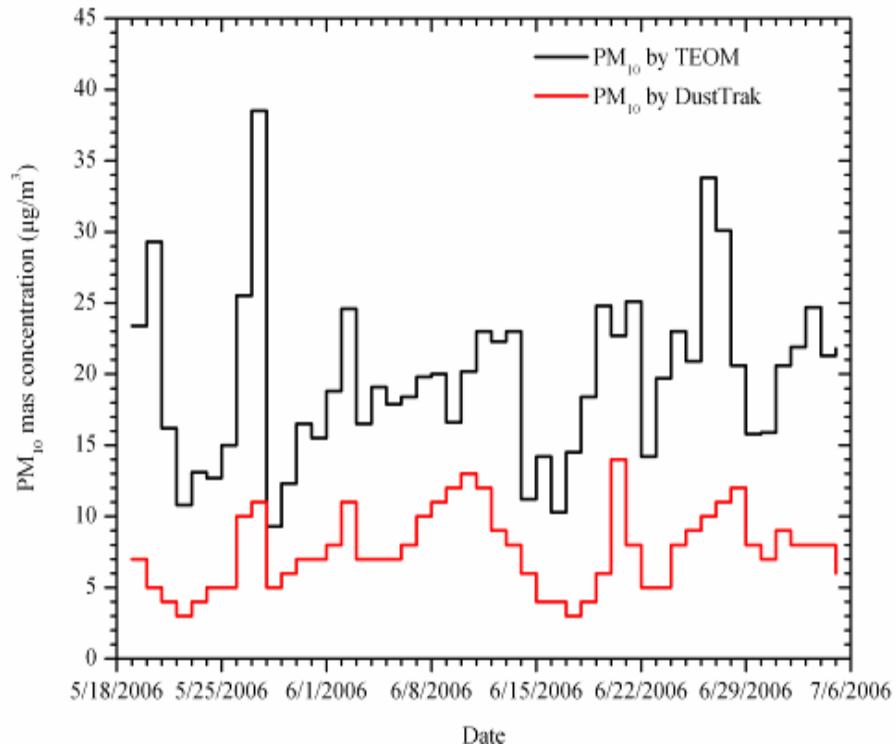


Figure 13. PM₁₀ mass (µg/m³) measured with DUSTTRAK and TEOM at Site #2 (Beatty).

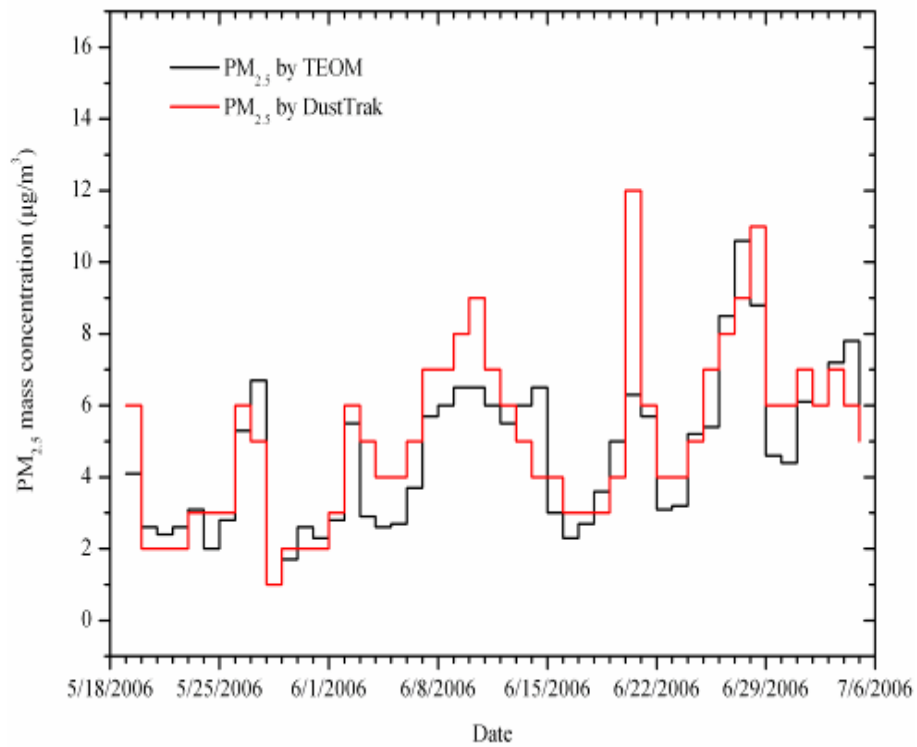


Figure 14. PM_{2.5} mass (µg/m³) measured with DUSTTRAK and TEOM at Site #2 (Beatty).

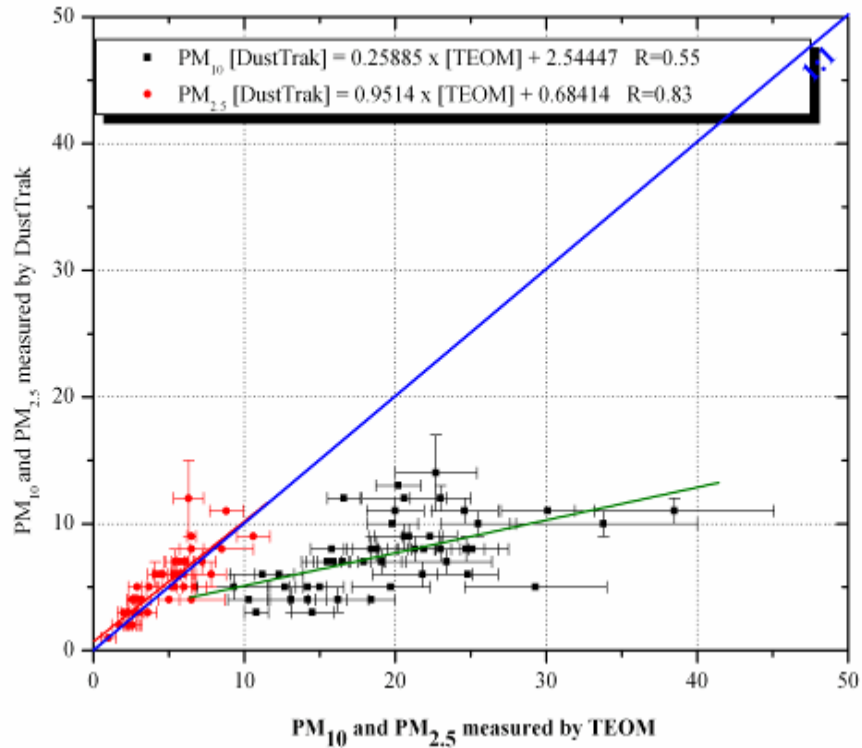


Figure 15. Comparison of 24-h PM_{10} and $PM_{2.5}$ mass concentrations measured by TEOM and DUSTTRAK. Error bars represent the standard error of the mean.

Comparison of Filter to Continuous Results

Figure 16 and Figure 17 show the relationships between PM_{10} and $PM_{2.5}$ measured by TEOM/DUSTTRAK and FRM filter-based methods. The temporal correlations between PM_{10} and $PM_{2.5}$ measurements by TEOM, DUSTTRAK, and filter methods were good, with correlation coefficients from 0.83 to 0.88. The slopes for TEOM and DUSTTRAK were 0.58795 and 0.43464. A high intercept was estimated for TEOM ($7.36477 \mu\text{g}/\text{m}^3$). The weak correlation between TEOM and filters was more pronounced for PM mass concentrations higher than $20 \mu\text{g}/\text{m}^3$. This may be due to the volatilization of organic carbon mass in the heated compartment. As for $PM_{2.5}$, TEOM, DUSTTRAK, and filter-based methods showed a very good agreement (slopes of 1.04491 and 1.18197, intercepts of 0.37547 and 0.36847 $\mu\text{g}/\text{m}^3$ for TEOM and DUSTTRAK, respectively).

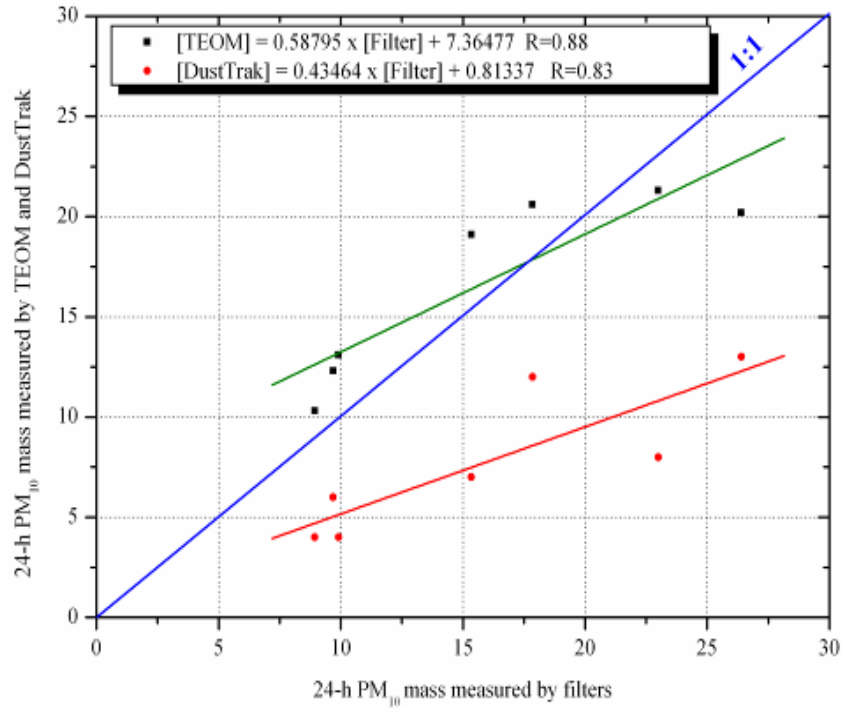


Figure 16. Relationships between PM₁₀ concentrations (µg/m³) measured by TEOM, DUSTTRAK, and filter-based methods.

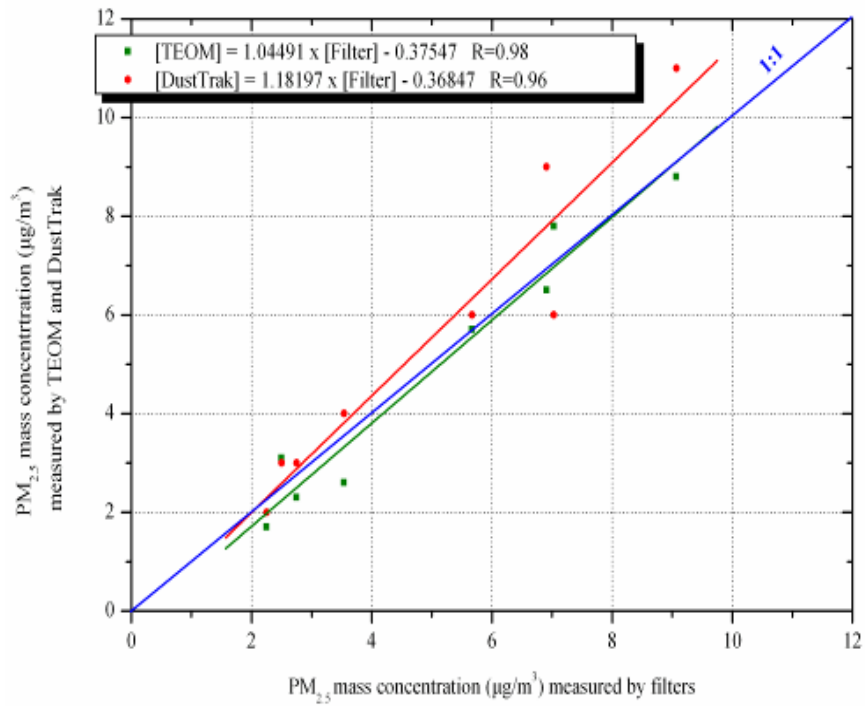


Figure 17. Relationships between PM_{2.5} concentrations (µg/m³) measured by TEOM, DUSTTRAK, and filter-based methods.

METEOROLOGY

Variations of hourly data for each meteorological parameter are presented in Figure 18 through Figure 22. Descriptive statistics of hourly data also are presented in Table 5. Solar radiation progressively increased up to 87.7 watts/m² (Figure 18). Ambient temperature varied from 42.3 to 103.9°F with a mean temperature of 77.8°F for the monitoring period (Table 5), which was associated with a decrease in relative humidity (Figure 19). During the monitoring period, two rain events occurred (Figure 20), with a total precipitation of 17.53 mm.

Table 5. Descriptive statistics of 1-hour meteorological data.

	Mean	Minimum	Maximum	Sum
Solar Radiation (watts/m ²)	28.6	0.0	87.7	
Wind speed (miles/h)	7.3	0.7	22.2	
Temperature (°F)	77.8	42.3	103.9	
Relative humidity (%)	20	7	78	
Precipitation (mm)				17.53

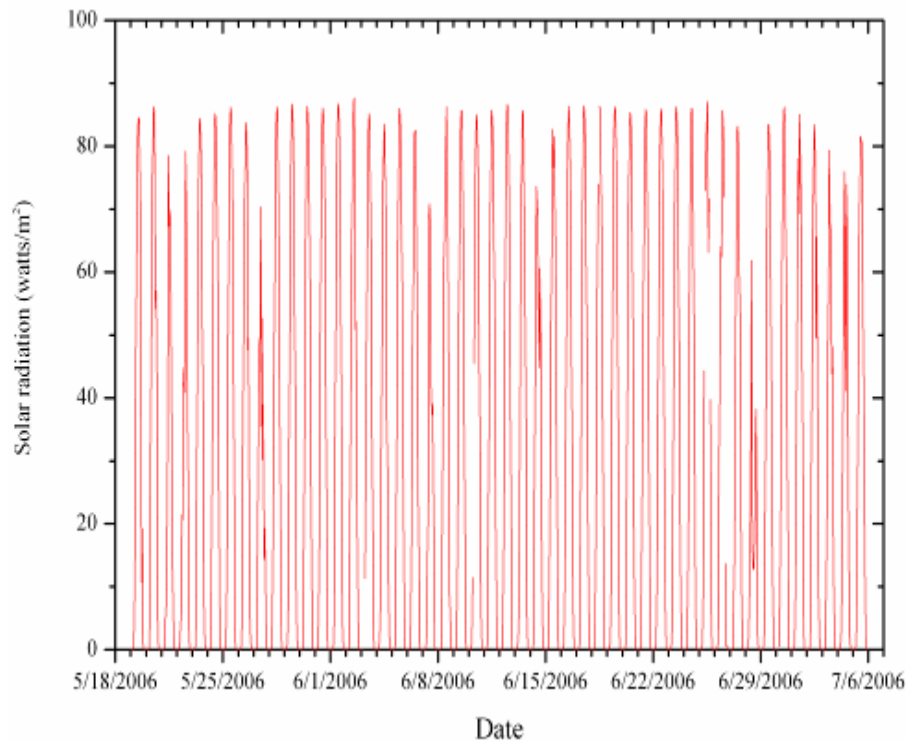


Figure 18. Solar radiation (in watts/m²) at Site #2 (Beatty).

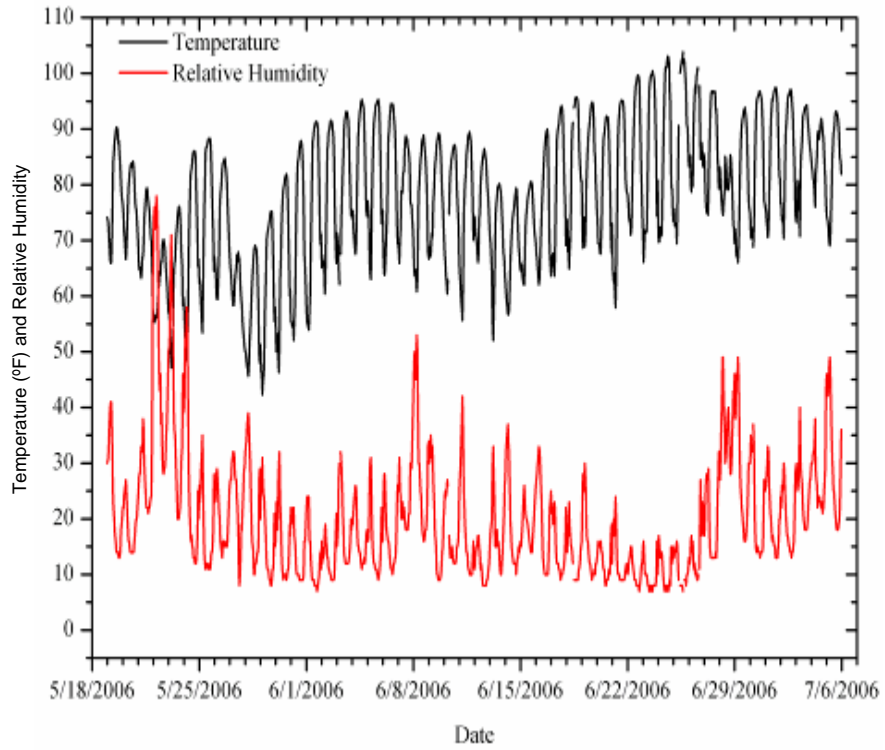


Figure 19. Temperature (in °F) and relative humidity at Site #2 (Beatty).

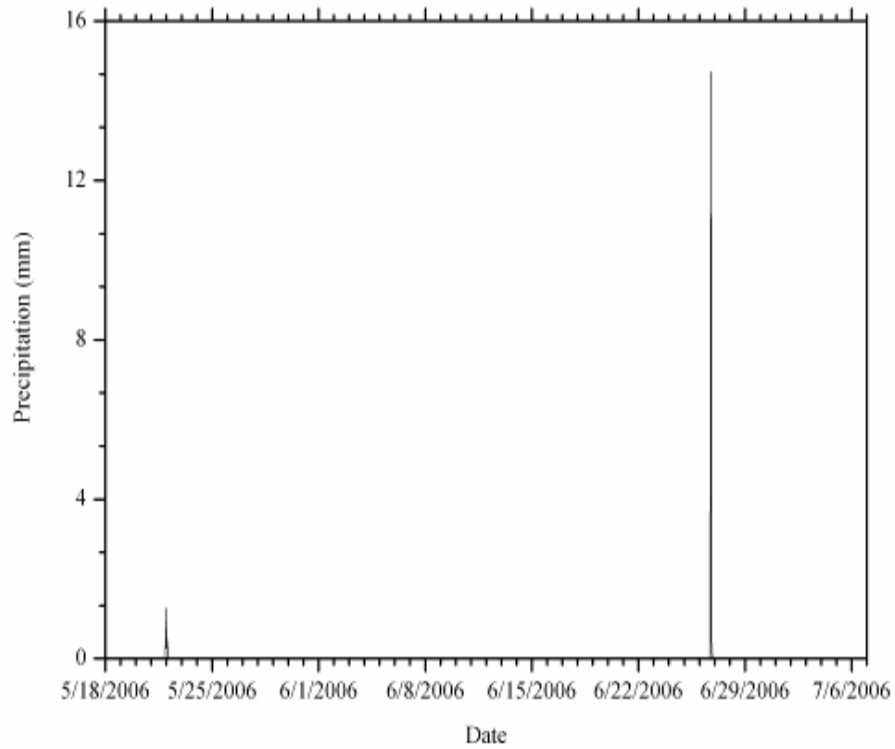


Figure 20. Total precipitation (in mm) at Site #2 (Beatty).

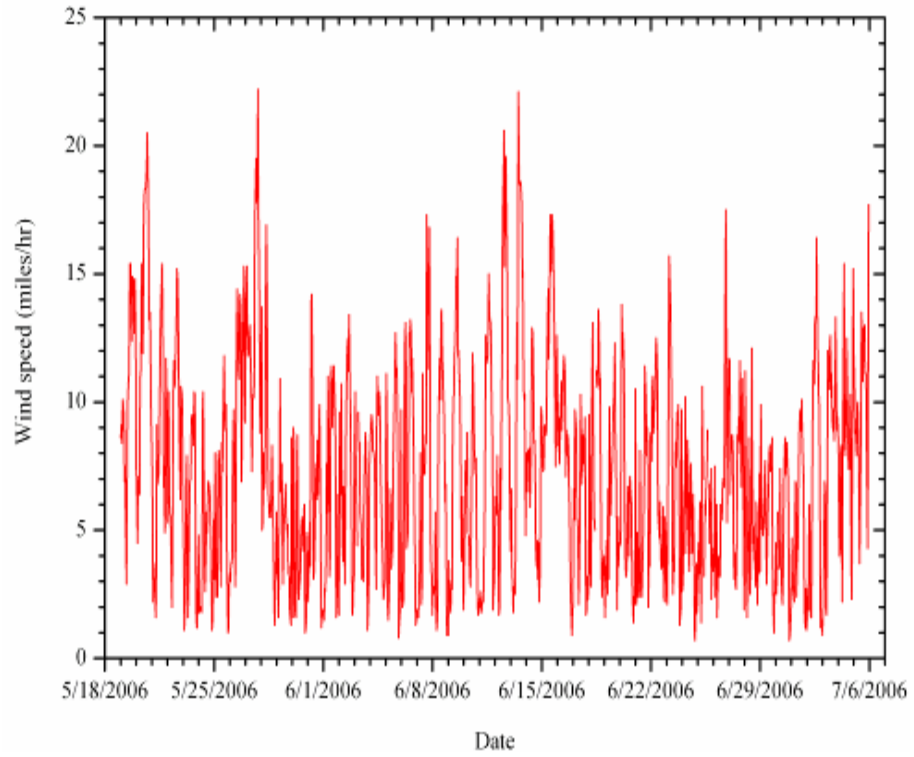


Figure 21. Wind speed (in miles/hr) at Site #2 (Beatty).

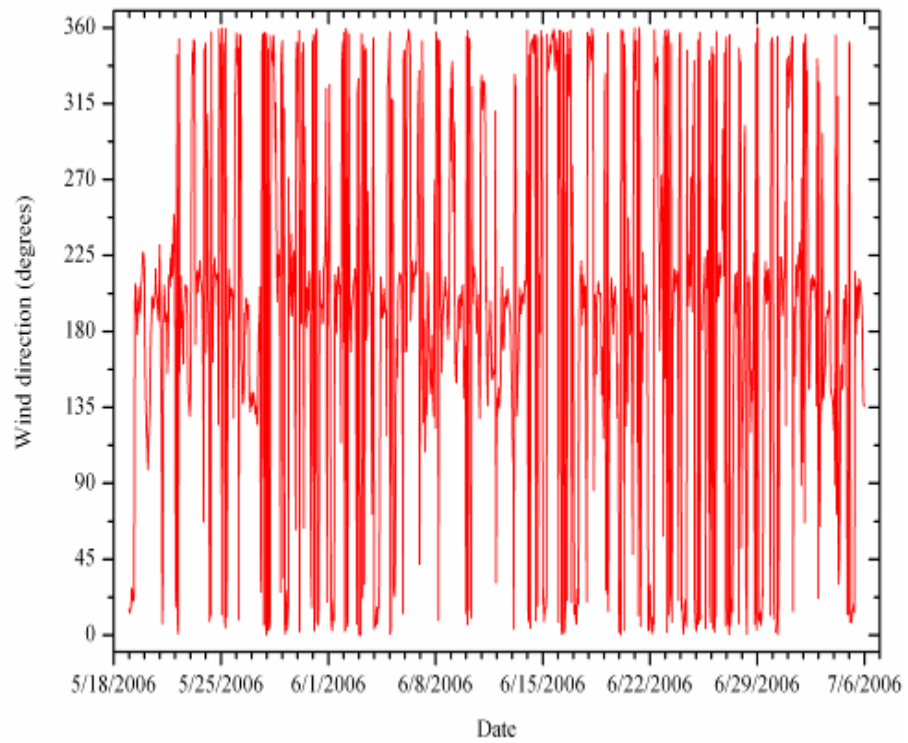


Figure 22. Wind direction at Site #2 (Beatty).

The monitoring period was described by frequent changes of the wind direction (north-south) with moderate wind speeds (Table 6; Figure 21 and Figure 22). To obtain information on prevailing winds, the polar plot of wind condition is given (Figure 23). The classification of wind conditions was retrieved from the Federal Meteorological Handbook (Table 6). The mean wind speed for each direction bin (16 bins) is presented in Figure 23.

Table 6. Wind condition classifications.

Miles/hour	Specification
<1	Calm; smoke rises vertically.
1 to 5	Direction of wind shown by smoke drift not by wind vanes. Wind felt on face; leaves rustle; vanes moved by wind.
5 to 9	Leaves and small twigs in constant motion; wind extends light flag.
9 to 14	Raises dust, loose paper; small branches moved.
14 to 23	Small trees in leaf begin to sway; crested wavelets form on inland waters. Large branches in motion; whistling heard in overhead wires; umbrellas used with difficulty.
23 to 35	Whole trees in motion; inconvenience felt walking against wind. Breaks twigs off trees; impedes progress.
35 to 48	Slight structural damage occurs. Trees uprooted; considerable damage occurs.
>48	Widespread damage.

(retrieved from Federal Meteorological Handbook; Chapter 5. Wind;
<http://www.nws.noaa.gov/oso/oso1/oso12/fmh1/fmh1ch5.htm#chp5link>)

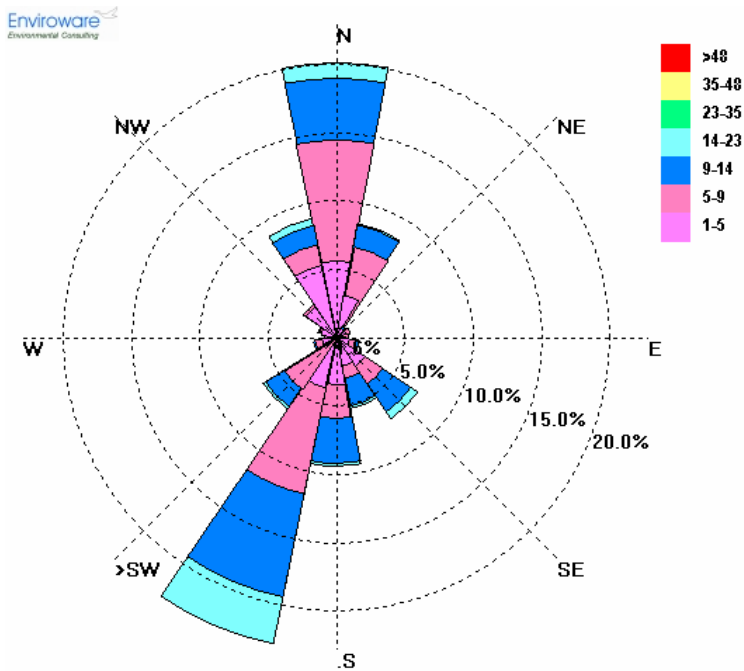


Figure 23. Wind direction and speed at Beatty.

For the entire monitoring period, the prevailing wind direction was north and southwest, with wind speeds lower than 23 miles/hour. More than 5 percent of southwest winds were associated with wind speeds higher than 14 miles/hour (mean wind speed ~9 miles/hour; Figure 24), which has been defined as the threshold for windblown dust emissions. Winds from the north sector were mostly associated with wind speed less than 14 miles/hour.

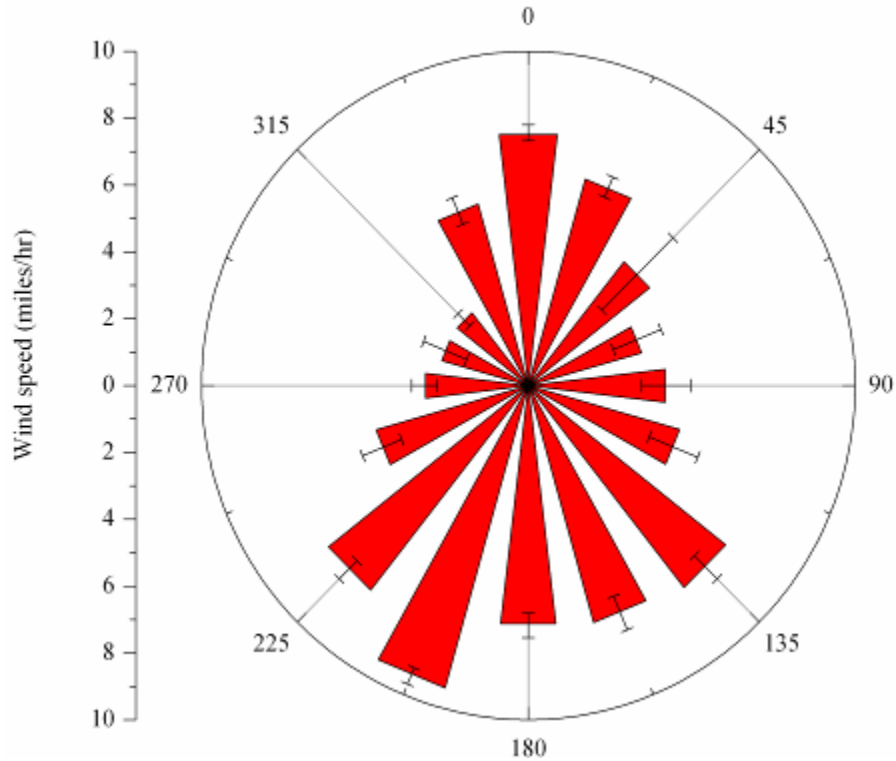


Figure 24. Average wind speed for each wind direction sector. Error bars represent the standard error of the mean.

Associations of Meteorology with Aerosol Measurements

The trends and correlations of PM mass with meteorological conditions are shown for hourly TEOM data. The increase in wind speed triggered higher PM₁₀ concentrations but a gradual decrease in PM_{2.5} concentrations. Both PM₁₀ and PM_{2.5} mass concentrations increased in early morning (6:00 to 8:00) and evening (18:00 to 20:00). These profiles indicated that traffic (local or on U.S. Highway 95) may be the most important source of fine particles, with higher winds resulting in faster transport/dilution. On the other hand, higher wind speeds also may induce higher emissions from potential sources of coarse particles (e.g., dust) in the area located in the northwest and to a lesser extent in northeast sectors (Figure 25 through Figure 27).

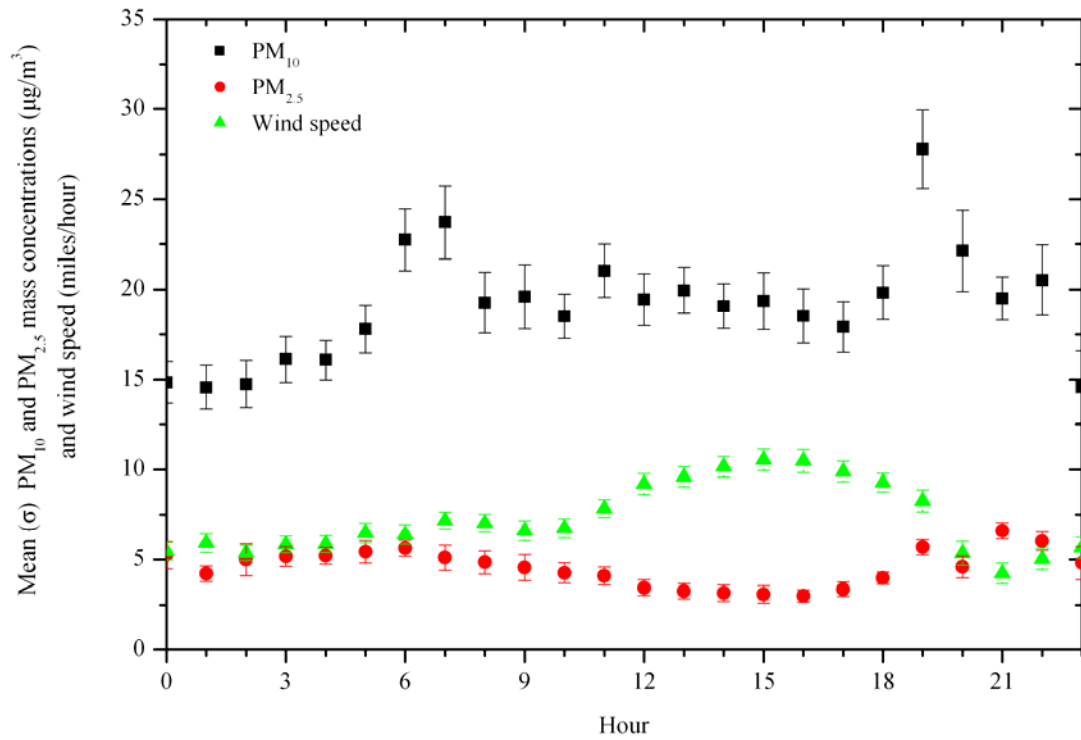


Figure 25. Hourly variation of PM₁₀ and PM_{2.5} mass concentrations ($\mu\text{g}/\text{m}^3$) as well as wind speed (miles/hour) at Site #2 (Beatty). Error bars represent the standard error of the mean.

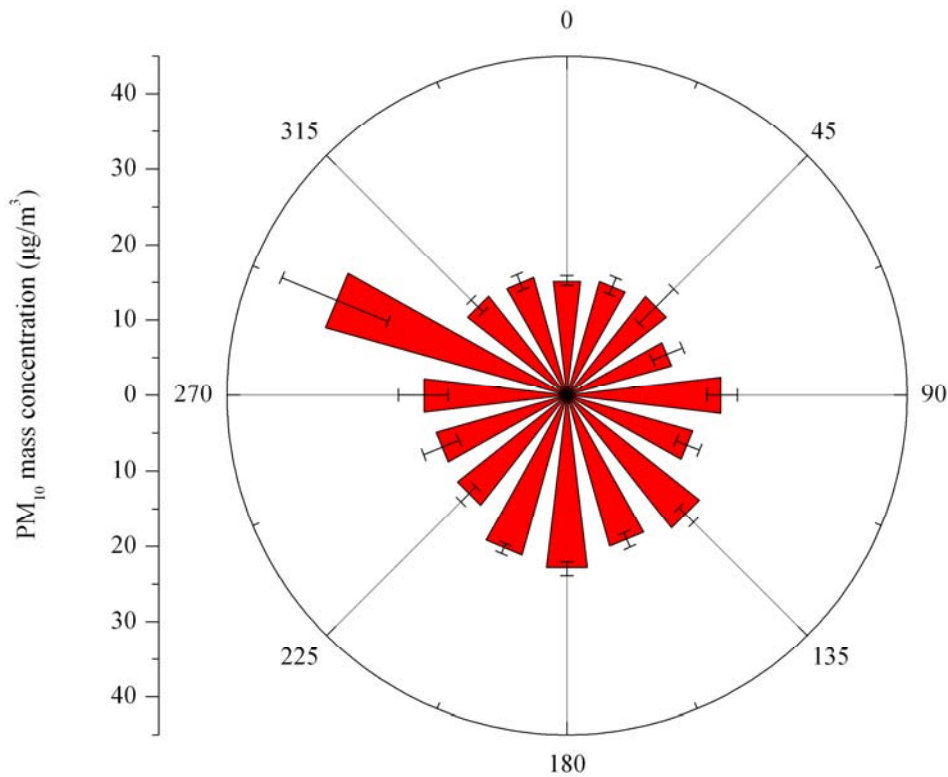


Figure 26. Mean (\pm st.error) of PM₁₀ mass concentrations ($\mu\text{g}/\text{m}^3$) for different wind direction sectors at Site #2 (Beatty).

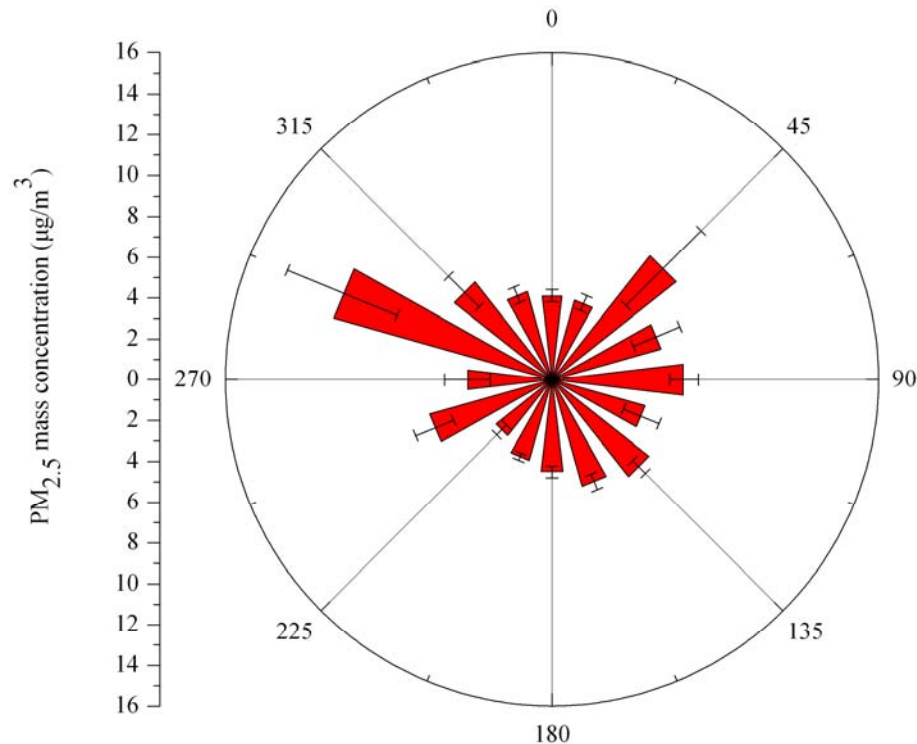


Figure 27. Mean (\pm st.error) of $PM_{2.5}$ mass concentrations ($\mu\text{g}/\text{m}^3$) for different wind direction sectors at Site #2 (Beatty).

CONCLUSIONS

PM_{10} and $PM_{2.5}$ mass concentrations and meteorological conditions were continuously monitored from May 18 to July 05, 2006, in Beatty, Nevada, with continuous (TEOM and DUSTTRAK) monitors. At the same time, integrated samples of PM_{10} and $PM_{2.5}$ were collected using FRM samplers on a 1-to-6-day schedule. Two sets of filters (June 4 and June 28, 2006) were analyzed for major anions (sulfate, nitrate, chloride) and cations (sodium and potassium), elements (from sodium to uranium), and elemental and organic carbon. The comparison of PM_{10} and $PM_{2.5}$ mass concentrations obtained by continuous monitors and filters showed that differences are associated with the limitations of the operating principle. For example, while light scattering (the measurement technique for DUSTTRAK) is not influenced by volatilization losses and it is accurate for fine particles, it performs poor for coarse particles, resulting in underestimation of PM_{10} mass. TEOM PM_{10} measurements were subject to volatilization artifacts at relatively high PM_{10} concentrations. $PM_{2.5}$ mass measurements obtained by TEOM, DUSTTRAK, and filter-based methods were comparable.

Mean 24-h concentrations of PM_{10} and $PM_{2.5}$ mass were 19.7 and $4.6 \mu\text{g}/\text{m}^3$, which are significantly lower than the 24-h and annual NAAQS standards (24-h PM_{10} : $150 \mu\text{g}/\text{m}^3$, 24-h $PM_{2.5}$: $35 \mu\text{g}/\text{m}^3$; Annual $PM_{2.5}$: $15 \mu\text{g}/\text{m}^3$). Higher PM_{10} and $PM_{2.5}$ mass concentrations during the weekend and in the early morning and late afternoon indicated the contribution of traffic emissions from U.S. Highway 95 and the town of Beatty. Comparatively higher PM_{10} levels (and decrease in $PM_{2.5}$ concentrations) were also associated with increased wind speeds blowing mostly from the north/northwest in early afternoon. This suggested strong

contribution of coarse particles from sources located north of the sampling site. The chemical composition of both PM₁₀ and PM_{2.5} samples indicated that organic carbon is the major component of both fractions, while soil contributes approximately 50 percent of PM₁₀ mass. Sulfate and nitrate account for about 15 percent. Increases in PM₁₀ and PM_{2.5} mass concentrations are associated with higher concentrations of organic mass. However, the importance of organic carbon mass may be overestimated, especially for fine particles, because of the absorption of low-vapor pressure organic gases by the quartz filter.

ACKNOWLEDGEMENTS

Authors thank Mr. John C. Lisle for hosting the mobile trailer on his property.

REFERENCES

- Kavouras, I.G., V. Etyemezian, D. DuBois, J. Xu, M. Pitchford, and M. Green. 2005. Assessment of the Principal Causes of Dust-Resultant Haze at IMPROVE Sites in the Western United States. Final report to Western Regional Air Partnership (www.coha.dri.edu/dust).
- Lefer, B.L. and R.W. Talbot. 2001. Summertime measurements of aerosol nitrate and ammonium at a northeastern U.S. site. *Journal of Geophysical Research*, 106, 20,365 – 20,378.
- Malm, W.C., B.A. Schichtel, R.B. Ames, and K.A. Gebhart. 2002. A 10-year spatial and temporal trend of sulfate across the United States. *Journal of Geophysical Research*, 107, 4627, doi:10.1029/2002JD002107
- Malm, W.C., B.A. Schichtel, M.L. Pitchford, L.L. Ashbaugh, and R.A. Eldred. 2004. Spatial and monthly trends in speciated fine particle concentration in United States. *Journal of Geophysical Research*, 109, D03306, doi:10.1029/2006JD003739.
- White, W.H. and P.T. Roderts. 1977. On the nature and origins of visibility-reducing aerosol in the Los Angeles air basin. *Atmospheric Environment*, 11, 803-812.